



Contents lists available at ScienceDirect

Journal of Pharmaceutical Analysis

journal homepage: www.elsevier.com/locate/jpa

Original article

Determination of inhibitory activity of *Salvia miltiorrhiza* extracts on xanthine oxidase with a paper-based analytical deviceXingchu Gong¹, Jingyuan Shao¹, Shangxin Guo, Jingjing Pan, Xiaohui Fan^{*}

Pharmaceutical Informatics Institute, College of Pharmaceutical Sciences, Zhejiang University, Hangzhou, 310058, China

ARTICLE INFO

Article history:

Received 10 April 2020

Received in revised form

20 September 2020

Accepted 20 September 2020

Available online 24 September 2020

Keywords:

Paper-based analytical device (PAD)

Point-of-care testing

Xanthine oxidase

Salvia miltiorrhiza extract

3D printing

ABSTRACT

A novel paper-based analytical device (PAD) was prepared and applied to determine the xanthine oxidase (XOD) inhibitory activity of *Salvia miltiorrhiza* extracts (SME). First, polycaprolactone was 3D printed on filter paper and heated to form hydrophobic barriers. Then the modified paper was cut according to the specific design. Necessary reagents including XOD for the colorimetric assay were immobilized on two separate pieces of paper. By simply adding phosphate buffer, the reaction was performed on the double-layer PAD. Quantitative results were obtained by analyzing the color intensity with the specialized device system (consisting of a smartphone, a detection box and sandwich plates). The 3D-printed detection box was small, with a size of 9.0 cm × 7.0 cm × 11.5 cm. Color component G performed well in terms of linearity and detection limits and thus was identified as the index. The reaction conditions were optimized using a definitive screening design. Moreover, a 10% glycerol solution was found to be a suitable stabilizer. When the stabilizer was added, the activity of XOD could be maintained for at least 15 days under 4 °C or –20 °C storage conditions. The inhibitory activity of SME was investigated and compared to that of allopurinol. The results obtained with the PAD showed agreement with those obtained with the microplate method. In conclusion, the proposed PAD method is simple, accurate and has a potential for point-of-care testing. It also holds promise for use in rapid quality testing of medicinal herbs, intermediate products, and preparations of traditional Chinese medicines.

© 2020 Xi'an Jiaotong University. Production and hosting by Elsevier B.V. This is an open access article under the CC BY-NC-ND license (<http://creativecommons.org/licenses/by-nc-nd/4.0/>).

1. Introduction

From ancient times until today, Chinese people have used herbal drugs for health maintenance and prevention and treatment of various diseases. The effectiveness and safety of traditional Chinese medicines (TCMs) are key factors in the quality control of TCMs [1]. At present, chemical composition analysis is used in the quality control of many TCMs [2,3]. However, analytical methods for the separation of the complex components of TCMs are sometimes difficult to develop, and typically require specific instruments, such as high-performance liquid chromatography (HPLC) and gas chromatography (GC) [4,5], which also makes detection costly. Moreover, TCMs present pharmacological effects through multiple targeting and integrative adjusting [6–8]. As a result, it is usually difficult to determine the internal effectiveness of TCMs just by

identifying several of their chemical constituents. Therefore, the bioactivity of TCMs may be used as quality indices [9,10]. Biological activities can be evaluated in cell, tissue, and animal models, which suffer from the disadvantages of large capital costs and long operation time. In conclusion, the development of effective and rapid methods for estimating the bioactivity of TCMs is of practical significance.

Currently, paper-based analytical devices (PADs) are gaining increasing attention worldwide due to their specific advantages of good portability, easy operation, reasonable cost, and rapid detection [11]. The method utilizes hydrophilic paper as a substrate material and creates hydrophobic barriers on it in order to generate functional areas. Common fabrication methods for PADs mainly include wax patterning [12], inkjet printing [13], photolithography [14], and paper cutting [15]. Most of these methods are simple, fast and capable of mass production. When reagents and samples are spotted on the test area, they can react and produce color or fluorescence, which can be quantitatively detected. Among the different types of signals, colorimetric signals are most commonly used owing to their simplicity, and the analysis is usually combined

Peer review under responsibility of Xi'an Jiaotong University.

^{*} Corresponding author.

E-mail address: fanxh@zju.edu.cn (X. Fan).

¹ The authors equally contributed to this work.

with practical and inexpensive equipment such as smartphones and scanners [16]. In biomedical applications of PADs, various approaches are adopted to generate color, including enzymatic assays [17], immunoassays [18], and nanoparticle-based assays [19]. To date, PADs have been widely applied in the concentration determination of many analytes, such as glucose [20], uric acid [21], and haptoglobin [22]. In general, PADs show potential applications in point-of-care (POC) testing according to the requirements of the ASSURED criteria, which dictate that POC tests should be affordable, sensitive, specific, user-friendly, rapid and robust, equipment-free, and deliverable to end-users [23,24].

There are several works on the activity determination of foods. Sharpe et al. [25] established a paper-based colorimetric method based on metal oxide nanoparticles to analyze antioxidant-containing samples in terms of their gallic acid equivalents. Nuchtavorn et al. [26] presented a novel method to create paper-based microfluidic devices (μ PADs) using a desktop digital craft plotter/cutter and technical drawing pens. They used PADs to measure the flavonoid and phenolic content and DPPH free radical scavenging activity in beverages including tea, wine, and beer samples.

There are also some reports on TCM activity determination with PADs. In a previous work, PADs were used to analyze the antioxidant activity of Danhong injection and its intermediates, providing a method to determine the biological activities of TCMs and their intermediates [27]. In another previous work, the inhibitory activity of mulberry extracts on α -glucosidase was also determined using PADs [28]. When PADs are integrated with bioassays for TCMs, there are several advantages. First, PADs can be used as a platform to measure the effects of TCMs on target enzymes, thus reflecting the efficacy of TCMs from a holistic perspective. Second, PADs have their own characteristics, such as low cost, easy operation, and convenient result readout, indicating that they are appropriate for performing bioassays for TCM quality evaluation. However, portable analytical systems for TCM activity determination have not been reported.

In this work, a portable PAD for the analysis of enzyme inhibitory activity of xanthine oxidase (XOD) was developed. XOD catalyzes the oxidation of hypoxanthine and xanthine to uric acid. Therefore, it is considered a therapeutic target for gout, which is a form of inflammatory arthritis characterized by tissue damage and associated with a high level of uric acid [29]. It was reported that many herbs, including *Salvia miltiorrhiza radix*, *Rhei radix*, *Polygoni cuspidati rhizoma*, *Selaginellae herba*, *Paeoniae radix rubra*, and *Ginkgo folium*, have anti-inflammatory effects and inhibit XOD activity [30]. Therefore, *Salvia miltiorrhiza* extracts (SME) were studied for their XOD inhibitory activity.

In this work, polycaprolactone-modified paper was fabricated via 3D printing and heating. Then, the modified paper was manually cut and functionalized with XOD, which could react with xanthine and nitroterazolium blue chloride (NBT) to induce a color change. A PAD with a double-layer structure was fabricated. A suitable color index was selected, and the reaction conditions were optimized by a definitive screening design. The best stabilizer was selected. Subsequently, the PAD with the optimum conditions was applied to analyze the bioactivities of SME samples, and the results were compared with those obtained via the conventional microplate method. The advantages of the present PAD method were also discussed.

2. Materials and methods

2.1. Materials

NBT (98%) and allopurinol (98%) were purchased from Aladdin Industrial Corp. (Shanghai, China). XOD and xanthine ($\geq 99\%$) were

purchased from Sigma-Aldrich Chemical Corp. (St. Louis, MO, USA). Ethylenediaminetetraacetic acid disodium salt dihydrate (EDTA- $2\text{Na}\cdot 2\text{H}_2\text{O}$, $\geq 99.0\%$), dipotassium hydrogen phosphate trihydrate ($\text{K}_2\text{HPO}_4\cdot 3\text{H}_2\text{O}$, $\geq 99.0\%$), potassium dihydrogen phosphate (KH_2PO_4 , $\geq 99.5\%$), and dextran (Mw 20,000) were purchased from Sinopharm Chemical Reagent Co., Ltd. (Shanghai, China). Glycerol (99%) was purchased from Shanghai Macklin Biochemical Co., Ltd. (Shanghai, China). Bovine serum albumin (BSA) was purchased from Absin Bioscience Inc. (Shanghai, China). Trehalose ($\geq 99\%$) was purchased from Sinozyme Biotechnology Co., Ltd. (Nanning, China). Ultrahigh-purity water was produced using a Milli-Q water purification system from Millipore (Milford, MA, USA). The 3D printing materials, namely, polycaprolactone, wax wire, and polylactic acid (PLA) filament, were purchased from Dongguan Top Cool Electronics Technology Co., Ltd. (Dongguan, China), Fuzhou Zhilei Electronic Technology Co., Ltd. (Fuzhou, China), and Hangzhou Shining 3D Technology Co., Ltd. (Hangzhou, China), respectively. *Salvia miltiorrhiza* (batch No. 170901) was purchased from Jiuzhou Drugstore (China Jo-Jo Drugstores Inc., Hangzhou, China).

2.2. Reagent preparation

The XOD solution was dissolved in phosphate buffer (PB), and the enzyme concentration was optimized. The buffer pH value was calibrated with a pH meter (SevenMulti, Mettler Toledo, Schwerzenbach, Switzerland) and adjusted to various values (7.0, 7.5 and 8.0) before use. Substrate solutions of xanthine (0.48 mM) and a stock solution of allopurinol (400 $\mu\text{g}/\text{mL}$) were prepared separately in the same PB solution. Allopurinol solutions with serial concentrations (10–100 $\mu\text{g}/\text{mL}$) were obtained by diluting the stock solution with an appropriate amount of the buffer solution. A 10% (V/V) glycerol solution was prepared with ultrahigh-purity water.

2.3. Sample preparation

First, 50 g of *Salvia miltiorrhiza* was extracted twice with water (first with 350 mL for 30 min and then with 300 mL for 20 min). Then, the extracts were merged for rotatory evaporation and concentrated to 250 mL. To prepare the samples for testing, PB solution (pH 8.0) was used to quantitatively dilute the SME samples.

2.4. Preparation of PAD

In brief, filter paper was first modified with polycaprolactone and then folded into a double-layer construction with simple paper cutting and origami steps. A schematic illustration of the fabrication process is presented in Fig. S1. A pre-designed pattern of the paper-based chip was drawn with 3D Builder software (Microsoft Corporation, USA), and the top view of the designed pattern is shown in Fig. S1A. Then, polycaprolactone was printed on Whatman No. 202 quantitative filter paper (Hangzhou Wohua Whatman Filter Paper Co., Ltd., Hangzhou, China) using a desktop 3D printer (Einstart-S, Hangzhou Shining 3D Technology Co., Ltd., Hangzhou, China), as shown in Fig. S1B. Next, the printed paper-based chip was placed into an electric baking pan (JK-3030S2, Joyoung Co., Ltd., Hangzhou, China) and heated at 150 °C for 90 min. Upon heating, polycaprolactone melted and penetrated through the paper to form hydrophobic barriers, as shown in Fig. S1C. After that, polycaprolactone-modified paper was cut to obtain two pieces, as shown in Fig. S1D.

The reagents were loaded onto the hydrophilic regions of the paper-based chips, as shown in Fig. S1E. A total of 20 μL of XOD solution and a certain volume of 10% glycerol solution were pipetted onto the reaction zone of one piece of paper (enzyme

layer). After drying at room temperature for 30 min, XOD was immobilized on the reaction region. A certain volume of xanthine solution and 20 μL of NBT were preloaded onto the reaction zone of another piece of paper (substrate layer) and air dried. After that, the PAD was obtained and available for the sample test.

2.5. Colorimetric reaction

The practical operation of the colorimetric reaction based on the PAD is displayed in Fig. 1. The two pieces of the PAD were combined to form a double-layer reaction structure in which the substrate layer was the upper layer, as shown in Fig. 1A. Afterwards, the PAD was mounted on a small support plate with a lid and several clips to clamp it. All of the reaction devices were made by 3D printing with wax wire as the printing material, as shown in Figs. 1B and C. When the reaction process was performed, since the enzyme and substrate solutions had already been immobilized onto the PAD during fabrication, the only reagent that needed to be added was buffer solution. Therefore, a certain volume of PB solution was added to the substrate layer so that it could penetrate down and accelerate the process of the enzymatic reaction. Once the reaction was completed, the substrate layer was separated from the enzyme layer, and then the paper-based chip was dried. The enzyme layer with a deeper color was selected to analyze the color intensity, while the substrate layer with a lighter color was unsuitable for color analysis, as shown in Fig. 1A.

2.6. Determination of colorimetric reaction results

After the enzymatic reaction was carried out, the color intensity of the enzyme layer was measured with two detection systems. The first is a homemade detection system we published previously [28]. The detailed information of this system can be found in Fig. S2.

Since the main purpose of this work was to provide a potential method for POC use, a detection device with a smaller size (9.0 cm \times 7.0 cm \times 11.5 cm) was designed and 3D printed with PLA filament, as presented in Figs. 2A–D. With the goal of reducing the

size and weight of the detection box, no LED light tubes were installed in it. Instead, flashlight of the smartphone was turned on to illuminate the paper-based chip. Moreover, the paper-based chip was fixed on the sandwich plates, and they were moved integrally so that the color data of each detection zone could be measured one by one.

The color intensity was quantified by an app (Color Grab, version 3.6.1, Loomatix Ltd.). It was designed to capture and digitize colors from the real-world to the color intensity of many color models (RGB, CMYK, HSV, etc.) instantly, which made it portable to analyze the results of the color reaction. The software run shot is shown in Fig. 2D. The average intensity of the circular area was obtained. Then, samples were analyzed using both detection systems, and the results were compared.

Experiments were carried out under a specific combination of conditions to determine the color index for purple. A total of 20 μL of XOD solution (0.05 U/mL) and 10 μL of 10% glycerin solution were spotted onto the enzyme layer and air dried at room temperature. Then, 10 μL of allopurinol in a serial concentration gradient (10, 20, 40, 60, and 80 $\mu\text{g}/\text{mL}$) was added separately and dried. Accordingly, 10 μL of PB solution (pH 7.5) was added as a blank control. For the substrate layer, 60 μL of xanthine (0.48 mM) and 20 μL of NBT (1.0 mg/mL) were dropped onto it and dried as well. Once the two layers were overlapped as shown above, 20 μL of PB solution (pH 7.5) was added to the substrate layer to trigger the enzymatic reaction. The paper-based device was placed at room temperature for 30 min to promote the reaction. Afterwards, the two layers were separated and allowed to dry at room temperature.

2.7. Stability experiments

BSA, dextran, trehalose, and glycerol have been reported as enzyme stabilizers for PADs [31,32]. Regarding the stability of XOD immobilized onto the reaction zones, experiments were carried out to screen a suitable stabilizer among BSA (5 mg/mL), dextran (2 mg/mL), trehalose (2.75 mg/mL) and 10% glycerol. First, 10 μL of solutions of different stabilizers were added to the circular hydrophilic

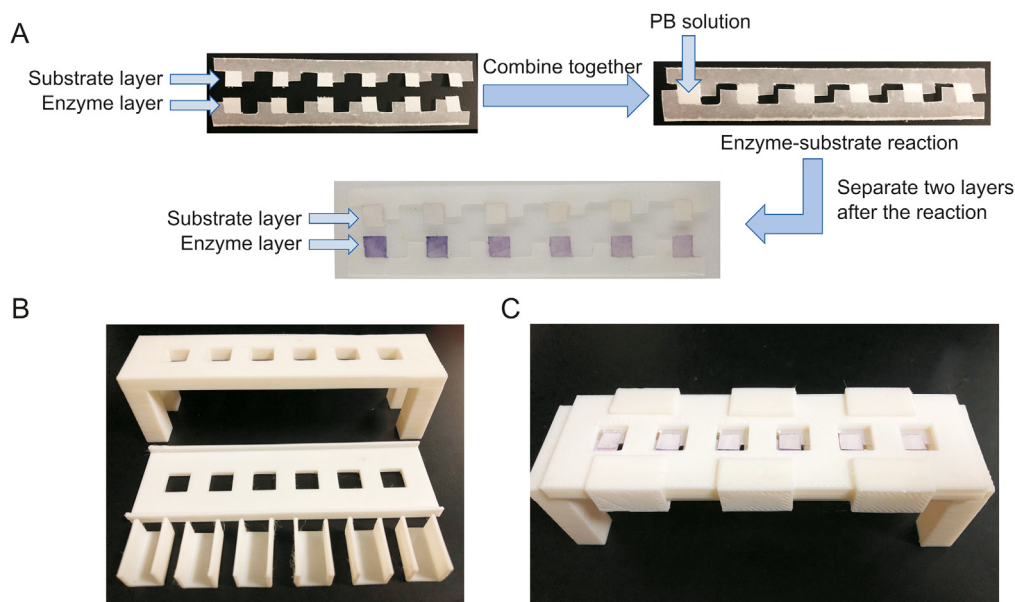


Fig. 1. Overall view of the reaction devices. (A) Practical demonstrations of colorimetric reactions based on PADs. The substrate layer and enzyme layer were overlapped after the reagents were added to each layer and dried. Then, PB solution was added to each test zone to trigger the enzymatic reaction. After the reaction, the two layers were separated, and the enzyme layer had a deeper color than the substrate layer. (B) All the device components were produced by 3D printing. (C) Demonstration of device operation while the enzymatic reaction was taking place.

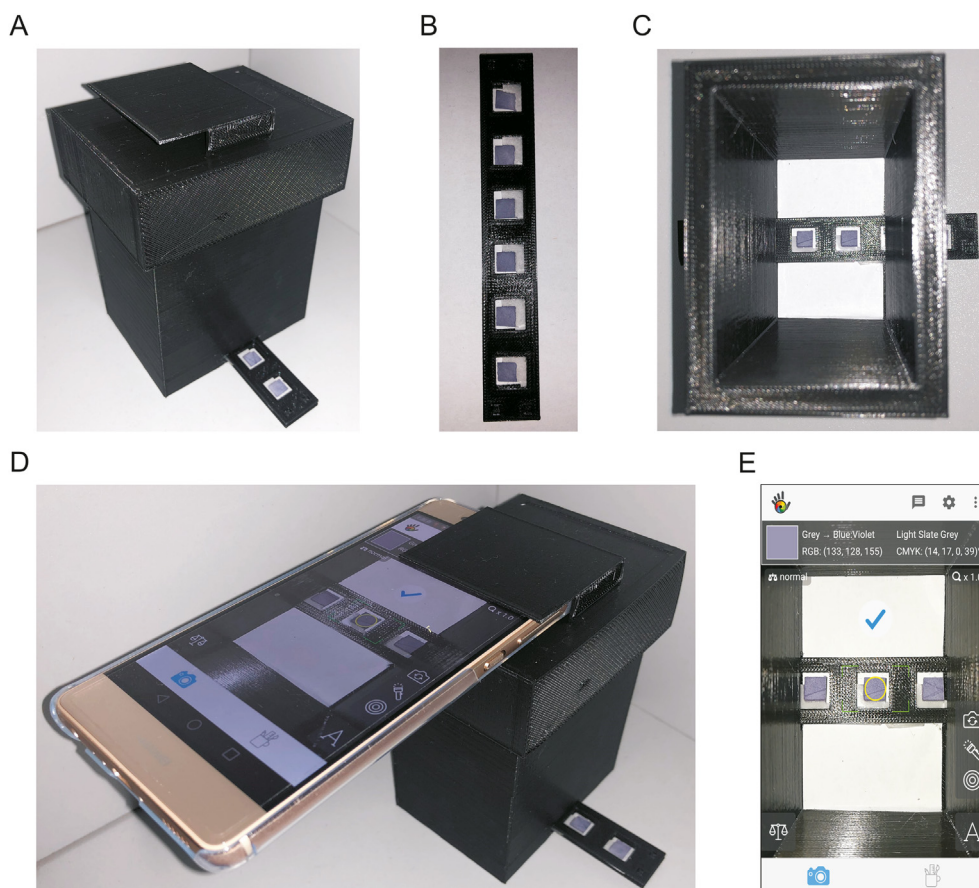


Fig. 2. Homemade detection devices and color capture process conducted with Color Grab software. (A) Device designed for POC use, (B) the sandwich plates, (C) the paper-based chip was placed on the sandwich plates and inserted into box, (D) the software was used to read the color intensity data in the detection zones, and (E) screenshot of the software while reading color intensity data.

paper-based zone. Then, 10 μL of XOD (0.05 U/mL) was added to each well. The mixed solution was air dried at room temperature for approximately 30 min. Afterwards, the paper-based chips with immobilized enzyme were separately stored in Petri dishes in two environments, one at room temperature (approximately 27 $^{\circ}\text{C}$) and the other at 4 $^{\circ}\text{C}$. Another set of paper-based chips containing stabilizers and XOD were kept frozen at -20°C . Paper-based chips in which the stabilizers were replaced with PB solution were prepared as controls. These chips were stored under these three conditions at the same time and tested for XOD activity. The activity of the immobilized XOD was tested after being stored for 1, 3, 5 and 7 days. First, 20 μL of xanthine (0.48 mM) and 10 μL of NBT (1.0 mg/mL) were added to each zone and left to react at room temperature for 30 min. Color component G was used to evaluate the stability of XOD. After the initial screening experiments, the activity of XOD with the best stabilizer was tested within 21 days.

2.8. Experimental design for the optimization of reaction conditions

Many factors may influence the results of the colorimetric reaction. The main influencing factors were investigated, including XOD concentration (X_1), 10% glycerol volume (X_2), xanthine volume (X_3), NBT concentration (X_4), PB solution volume (X_5), PB solution pH (X_6), reaction time (X_7), reaction temperature (X_8), and drying temperature (X_9). The coded and uncoded values of each parameter are listed in Table 1. A 25-run definitive screening design was employed to optimize the reaction parameters, as shown in Table S1. According to preliminary experiments, the concentration

Table 1
Parameters and their levels for the definitive screening design.

Parameter	Symbol	Coded value		
		-1	0	1
XOD concentration (U/mL)	X_1	0.05	0.1	0.15
10% glycerol volume (μL)	X_2	5	10	15
Xanthine volume (μL)	X_3	40	50	60
NBT concentration (mg/mL)	X_4	0.5	1	1.5
PB solution volume (μL)	X_5	15	20	25
PB solution pH	X_6	7	7.5	8
Reaction time (min)	X_7	20	30	40
Reaction temperature ($^{\circ}\text{C}$)	X_8	25	30	35
Drying temperature ($^{\circ}\text{C}$)	X_9	35	40	45

or volume of the main reagents was fixed as follows: XOD volume of 20 μL , xanthine concentration of 0.48 mM, and NBT volume of 20 μL .

2.9. Data analysis

Analysis of variance (ANOVA) was used to analyze the results of the definitive screening design. Quadratic models were built to evaluate the effects of parameters on each response according to Equation (1). The corrected Akaike information criterion (AICc) with backward selection was used to help simplify the model. The analysis of the results was performed using Design Expert software (version 10.0.4, Stat-Ease Inc., USA).

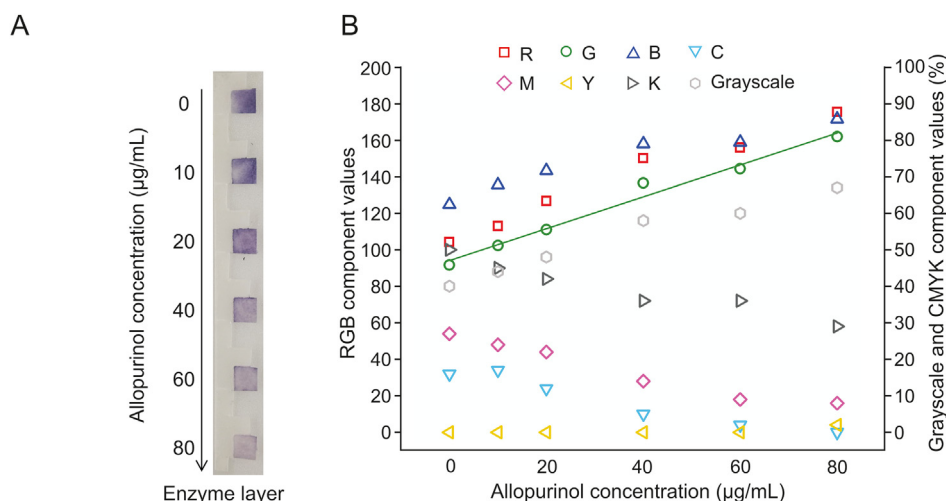


Fig. 3. Effects of allopurinol concentration on color intensity in the detection zones. (A) Photograph of the enzyme layer, and (B) scatter graph of color index values with allopurinol concentrations ranging from 0 to 80 µg/mL.

$$Y = a_0 + \sum_{i=1}^9 a_i X_i + \sum_{i=1}^9 a_{ii} X_i^2 + \sum_{i=1}^8 \sum_{j=i+1}^9 a_{ij} X_i X_j \quad (1)$$

where Y represents the measured values of the response, which is color component G in the RGB color model; a_0 is a constant; a_i , a_{ii} and a_{ij} represent the regression coefficients for the linear, quadratic, and interaction terms, respectively; and X represents each parameter. By applying multivariate regression analysis, an optimized condition was obtained and adopted for subsequent determination of the inhibitory effects of allopurinol and samples on XOD.

2.10. Model validation and method application

Three operation points were selected for model validation experiments to ensure that the measured response values agreed with the predictive results obtained from Equation (1). The experimental conditions are presented in Table S2. Subsequently, the optimum method was applied to quantitatively measure the XOD inhibitory activity of SME. Allopurinol solution was used as a positive control. After the addition of 10% glycerol and XOD, 10 µL of sample or allopurinol solution was separately dropped onto the enzyme layer and then air dried. The color intensity was closely related to the content of inhibitors, and the purple color decreased as the inhibitor content increased. Therefore, a calibration curve was established by plotting the color intensity values versus the inhibitor concentrations. The limit of detection (LOD) and limit of quantitation (LOQ) were separately calculated by Equation (2) and Equation (3) using OriginPro 2018 (OriginLab Corp., Northampton, MA, USA).

$$LOD = 3.3\sigma/S \quad (2)$$

$$LOQ = 10\sigma/S \quad (3)$$

where σ is the standard deviation of the response and S is the slope of the calibration curve. After that, the inhibitory effects of the samples were compared to that of allopurinol at certain concentrations.

2.11. Active component of SME and selectivity of the PAD method

To verify the active component of SME, the XOD inhibitory capacity of salviannic acid B solution was tested by the optimized PAD method. And the concentration of salviannic acid B solution was the same as that of SME. On the other hand, SME contains high levels of sugars, mainly including glucose, fructose, and sucrose [33]. And it is not reported that sugars can inhibit XOD. Therefore, in order to evaluate the selectivity of the PAD method, the XOD inhibitory capacity of the mixed solution consisting of 0.624 mg/mL fructose, 1.152 mg/mL glucose, and 1.564 mg/mL sucrose was studied. Sugar contents of SME were consulted from the literature [33]. Moreover, PAD without any sample solutions served as blank control.

3. Results and discussion

3.1. Preparation of polycaprolactone-modified paper

In this work, to prevent the colorimetric reaction of the enzyme and substrate during the storage of the PAD, the enzyme and substrate were added to two different hydrophilic zones and dried in advance. After the samples interacted with the enzymes, the two reaction zones were overlapped, and the reaction began when the buffer was added. In another design of the paper-based chip, in the center of the rectangle, the hydrophobic barrier was a hydrophilic enzyme reaction area, as shown in Fig. S3A. After these two pieces were folded and brought into contact with each other to form a square reaction area, as shown in Fig. S3B, the liquid tended to overflow when the PB solution was added.

To avoid sample leakage, an improved design pattern was developed before analysis of SME samples, as illustrated in Fig. S1. Detailed views of the present paper-based chip design are shown in Fig. S4. The basic building block of the hydrophobic barriers was an asymmetrical T-shaped structure, as shown in Fig. S4A. The blank space on one side was a defined square with a side length of 6.0 mm, while the other side was to be cut off, as displayed in Fig. S4B. Every two pieces of these blocks were combined together, and the polycaprolactone-covered boundary was made as an incomplete rectangle. Therefore, the center region without polycaprolactone was the reaction zone. Drawings of the combination of the two sheets of the PAD are shown in Fig. S4C. With this design, additional sample liquid could be added without risking exudation,

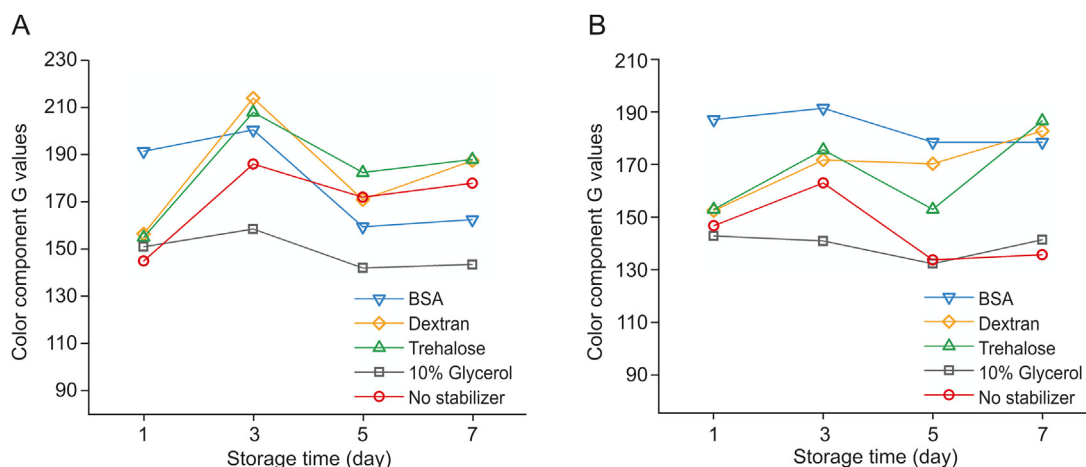


Fig. 4. Influence of stabilizers on the stability of XOD in two storage environments over 7 days. (A) Stored at 4 °C, and (B) stored at -20 °C.

thus improving the detection sensitivity of the PAD.

3.2. Selection of color index

The effects of allopurinol solutions with different concentrations on the color space parameters (RGB, CMYK and grayscale) were investigated. A photograph of the paper-based chip after the colorimetric reaction and the color intensity variations are shown in Fig. 3. For samples with higher XOD inhibitory activity, a weaker color was observed in the detection areas. With increased allopurinol concentration, the R value increased from 107 to 180, while the G value increased from 94 to 166. These two responses showed a consistent change trend. Other indexes (including B, C, M and grayscale value) varied within smaller ranges. The Y value remained near zero. Moreover, the LOD value calculated for the G index was the lowest. A large slope of the variation curve and a low LOD indicated an increase in the method sensitivity. Consequently, color component G was selected as the color index because of the linearity, slope, and LOD.

3.3. Stability of the PAD

The initial screening experiments of several stabilizers were carried out. A higher component G value indicated a greater decrease in the activity of XOD. We tested the paper-based chips kept at room temperature for three days to screen for the appropriate stabilizer. It was observed that XOD with the tested stabilizers clearly lost activity. Then, the other two storage environments (4 °C and -20 °C) were used, and the results are shown in Fig. 4. These results showed that XOD with 10% glycerol maintained enzyme activity for 7 days, while the effects of the other stabilizers were unsatisfactory.

Next, the stability of XOD with 10% glycerol for 21 days was tested, and the results are displayed in Fig. 5. When the paper-based chip was frozen at -20 °C, the G values remained nearly unchanged. However, XOD lost its activity gradually when stored at room temperature or at 4 °C without a stabilizer. Under 4 °C storage conditions, XOD containing 10% glycerol could retain its activity without any obvious changes in color component values during 15 days. After 21 days, however, XOD activity was obviously decreased. Therefore, 10% glycerol could help enhance the shelf life of paper-based chips preloaded with XOD to some extent.

3.4. Parameter optimization and method validation

The results of the definitive screening design experiments are shown in Table S1. The stepwise regression model of the color index was developed using the coded values of each parameter. For color component G, the equation was established as $Y=145.72-17.73X_2-4.59X_4-4.59X_5-23.59X_6-8.55X_7-9.75X_2X_3$ with a determination coefficient (R^2) of 0.9249 and an adjusted R^2 value of 0.8998. A high R^2 value means that most of the variations in the experimental data could be explained by the equation. Moreover, according to the coefficients of each factor in these two models, factors including 10% glycerol volume, NBT concentration, PB solution volume, PB solution pH and reaction time all showed negative correlations with the color index.

The results of the validation experiments are listed in Table S2. The validation results proved that the experimental values of color component G were close to the predicted values. This finding indicated that the model had a good predictive ability. When less XOD and xanthine were added, the cost of the device would be decreased. Moreover, with a shorter reaction time and lower temperature, the efficiency of the method would be increased. Therefore, the optimal conditions were determined as follows: XOD concentration of 0.05 U/mL, 10% glycerol volume of 15 μ L, xanthine volume of 60 μ L, NBT concentration of 1.5 mg/mL, PB solution volume of 25 μ L, PB pH of 8.0, reaction time of 30 min, reaction temperature of 25 °C, and drying temperature of 35 °C.

The XOD inhibitory activity of allopurinol solutions with different concentrations was measured with the optimized method. The range of calibration curve was 10–80 μ g/mL. The G value and allopurinol concentration were found to be related as $Y=1.2277X_1-151.96$. LOD and LOQ were calculated to be 10.9 μ g/mL and 32.9 μ g/mL, respectively. To further confirm the accuracy of the method, spike recovery experiments were performed at concentration levels of about 50%, 100%, and 150% of SME samples. The inhibitory effects of the SME samples were converted to allopurinol equivalents. As shown in Table S3, the average recoveries of samples were in the range between 87.06% and 109.95%, proving that the PAD method could achieve accurate results.

4. Discussion

4.1. Comparison with conventional methods

PAD and the conventional microplate method was adopted to examine whether XOD was inhibited by SME samples. The SME was

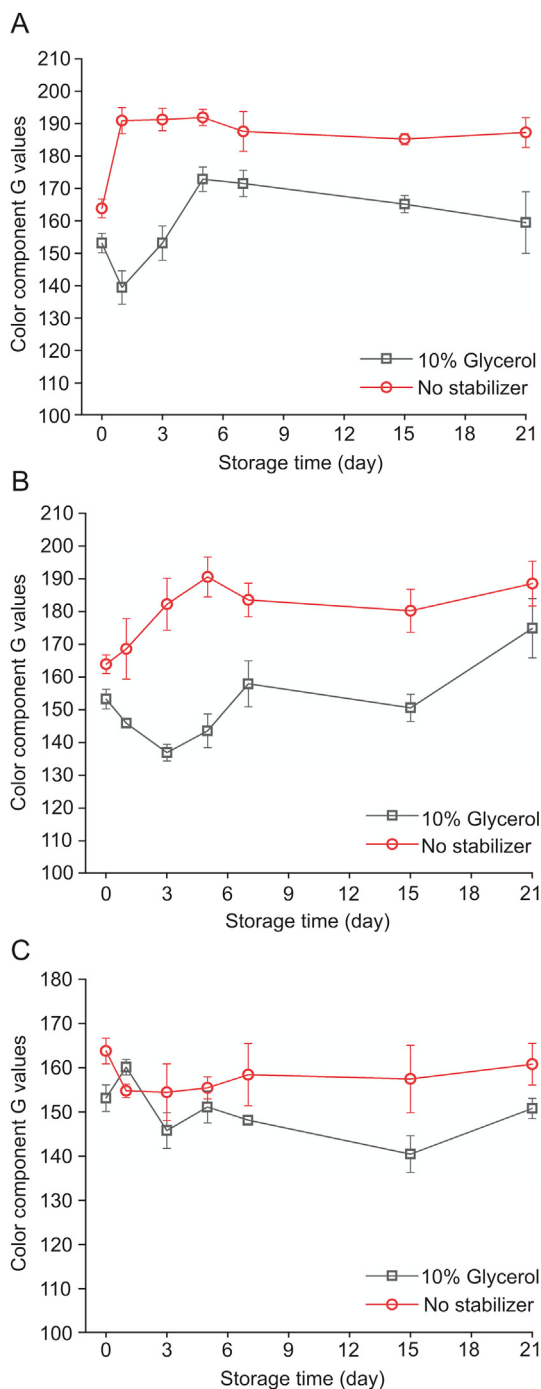


Fig. 5. Influence of 10% glycerol solution on the stability of XOD in three storage environments over 21 days. (A) Stored at room temperature, (B) stored at 4 °C, and (C) stored at -20 °C.

diluted with PB solution to 1/8–1/40 with three different concentrations. The color of samples was light. A blank control without XOD solution was added in each measurement. The color component values of samples were calculated by subtracting the values of blank control. In this way, PAD results would not be interfered by the color of tested samples. The results are shown in Fig. 6. There was no significant difference (Friedman test, $P=0.368$) among the three methods, which indicated the reliability of the PAD method.

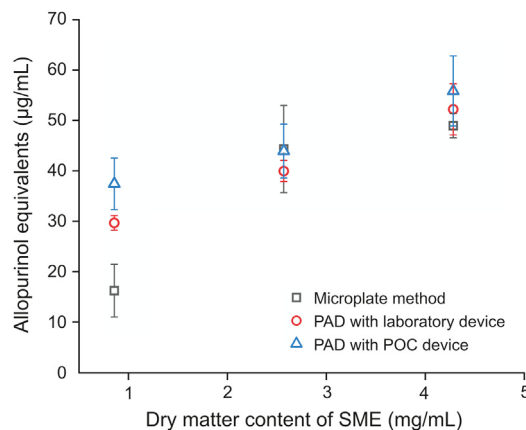


Fig. 6. Comparison of the inhibitory effects of SME samples obtained with the microplate assay and PAD methods.

4.2. Active component of SME and selectivity of the PAD method

The results of the active component verification and selectivity experiments are shown in Fig. S5. The color component G values of PAD were measured, and the results of these four groups from left to right were 56, 116, 99, and 59, respectively.

The G values of SME group and salvianolic acid B solution group were both significantly higher than that of the blank control group. It shows that both the SME and salvianolic acid B solution can inhibit the XOD activity. In other words, salvianolic acid B is one of the active components of SME which can effectively inhibit XOD. It is consistent with the results reported in the literature [34]. There was no significant change in the color between mixed sugar solution group and the blank control group. It means that the mixed sugar solution has little effect on the XOD activity, which proves the selectivity of the PAD method proposed.

4.3. Potential applications of the present technology

There are many advantages of the conventional microplate method. For example, the repeatability of analysis results is usually good. Because the solutions used for microplate analysis is often prepared before use, there is no need to worry about the stability of the solutions at most occasions. However, a microplate reader is required to determine the results of microplate method. The microplate reader is usually not cheap, and inconvenient to move. These disadvantages limit the applications of microplate method for onsite analysis.

In this work, the 3D-printed devices used in the PAD analysis were small. The size of the detection box was 9.0 cm × 7.0 cm × 11.5 cm, while the size of the reaction support device was 13.0 cm × 3.5 cm × 3.9 cm. Smartphones are very popular in China. Therefore, these PADs may be a powerful tool for the rapid quality testing of TCMs onsite during harvest and collection periods. Because the 3D-printed devices used in the PAD analysis are also cheap, the present method is promising in allowing users to conveniently assess the bioactivity of homemade herbal decoctions at home. The decision on harvesting a herbal material or taking a decoction can be made rapidly. Compared with conventional microplate method, microplate reader was not required, which further lowers the cost of analysis. Because enzyme, substrate, and chromogenic reagent are dried on PADs in advance, only sample solution and PB solution are required in the analysis, which reduces the workload through adding less kinds of solutions in the reaction system.

SME is also the intermediate of many TCM preparations, such as Danshen injection. Quality analysis requiring long time is not suitable for industrial intermediates. The present method could also be used to control the quality of production intermediates of TCMs. Furthermore, PADs with certain enzymes immobilized on them for POC food bioactivity determination can be accessible.

As a bioassay method, the advantage of the present PAD method is evaluating the TCM quality in general. However, the specificity of bioassay of TCMs is usually lower than that of chemical analysis methods, such as the chemical fingerprint method [6]. Therefore, bioassay is usually considered as a supplement to the current TCM quality evaluation mode [6]. When using the PAD method to determine TCM quality, the identification of medicinal herbs according to their appearance can improve the specificity.

5. Conclusion

An XOD activity assay method was developed using an optimized paper-based device. In this work, 3D printing, paper cutting, and folding methods were used to create the double-layer structure PAD. The enzymatic reactions resulted in color intensity variations, which were recognized and distinguished by color component G. Next, a definitive screening design was employed to optimize the reaction conditions. The PAD method was proven to be accurate by the sample spike experiments. Under the optimal conditions, the effects of SME on XOD were tested by PAD with two different detection devices and the microplate method at the same time. The stability experiments showed that the PAD with immobilized enzymes could be stored for at least 15 days without a decrease in activity after adding 10% glycerol under 4 °C or –20 °C storage conditions. Salvianolic acid B in SME possessed the ability to inhibit XOD activity. Furthermore, all the reaction and detection devices were of small size, making them portable and easy for operators to carry and use. Thus, the PAD offers a POC platform for the convenient measurement of XOD inhibitory activity. The present method is promising in POC analysis.

Declaration of competing interest

The authors declare that there are no conflicts of interest.

Acknowledgments

The authors would like to thank the support of the National S&T Major Project of China (Grant No.: 2018ZX09201011), the National Natural Science Foundation of China (Grant No.: 81503242), and the Fundamental Research Funds for the Central Universities (Grant No.: 2018FZA7018).

Appendix A. Supplementary data

Supplementary data to this article can be found online at <https://doi.org/10.1016/j.jpha.2020.09.004>.

References

- [1] C.X. Liu, Recognizing healthy development of Chinese medicine industry from resources quality-quality markers of Chinese medicine, *Chin. Tradit. Herb. Drugs* 47 (2016) 3149–3154.
- [2] Z.H. Li, X.H. Zhang, J. Liao, et al., An ultra-robust fingerprinting method for quality assessment of traditional Chinese medicine using multiple reaction monitoring mass spectrometry, *J. Pharm. Anal.* 11 (2021) 88–95.
- [3] Z.Z. Yang, J.Q. Zhu, H. Zhang, et al., Investigating chemical features of Panax notoginseng based on integrating HPLC fingerprinting and determination of multiconstituents by single reference standard, *J. Ginseng Res.* 42 (2018) 334–342.
- [4] S.P. Li, J. Zhao, B. Yang, Strategies for quality control of Chinese medicines, *J. Pharmaceut. Biomed. Anal.* 55 (2011) 802–809.
- [5] X.M. Liang, Y. Jin, Y.P. Wang, et al., Qualitative and quantitative analysis in quality control of traditional Chinese medicines, *J. Chromatogr. A* 1216 (2009) 2033–2044.
- [6] Y. Jiang, B. David, P.F. Tu, et al., Recent analytical approaches in quality control of traditional Chinese medicines: a review, *Anal. Chim. Acta* 657 (2010) 9–18.
- [7] D.Y. Yu, P.L. Zhang, J.Y. Li, et al., Neuroprotective effects of Ginkgo biloba dropping pills in Parkinson's disease, *J. Pharm. Anal.* 11 (2021) 220–231.
- [8] Y.Y. Li, X.Y. Lu, J.L. Sun, et al., Potential hepatic and renal toxicity induced by the biflavonoids from Ginkgo biloba, *Chin. J. Nat. Med.* 17 (2019) 672–681.
- [9] C. Zhang, X. Zheng, H. Ni, et al., Discovery of quality control markers from traditional Chinese medicines by fingerprint-efficacy modeling: current status and future perspectives, *J. Pharmaceut. Biomed. Anal.* 159 (2018) 296–304.
- [10] X.H. Xiao, J.B. Wang, D. Yan, Studies and application of biological evaluation in the quality standardization of Chinese medicines, *Mod. Tradit. Chin. Med. Mater. Med-World Sci. Technol.* 16 (2014) 514–518.
- [11] Y. Lu, W.W. Shi, J.H. Qin, et al., Fabrication and characterization of paper-based microfluidics prepared in nitrocellulose membrane by wax printing, *Anal. Chem.* 82 (2009) 329–335.
- [12] K. Yamada, K. Suzuki, D. Citterio, Text-displaying colorimetric paper-based analytical device, *ACS Sens.* 2 (2017) 1247–1254.
- [13] P. Bezuidenhout, S. Smith, T.H. Joubert, A low-cost inkjet-printed paper-based potentiostat, *Appl. Sci. (Basel)* 8 (2018), 968.
- [14] H. Asano, Y. Shiraiishi, Microfluidic paper-based analytical device for the determination of hexavalent chromium by photolithographic fabrication using a photomask printed with 3D printer, *Anal. Sci.* 34 (2018) 71–74.
- [15] Y.S. Kim, Y. Yang, C.S. Henry, Laminated and infused Parafilm®-paper for paper-based analytical devices, *Sensor. Actuator. B Chem.* 255 (2018) 3654–3661.
- [16] D.M. Cate, J.A. Adkins, J. Mettakoonpitak, et al., Recent developments in paper-based microfluidic devices, *Anal. Chem.* 87 (2015) 19–41.
- [17] P. Kaewarsa, W. Laiwattanapaisal, A. Palasuwan, et al., A new paper-based analytical device for detection of Glucose-6-phosphate dehydrogenase deficiency, *Talanta* 164 (2017) 534–539.
- [18] T. Mazzu-Nascimento, G.G. Morbioli, L.A. Milan, et al., Improved assessment of accuracy and performance indicators in paper-based ELISA, *Anal. Methods* 9 (2017) 2644–2653.
- [19] C.W. Yen, H. de Puig, J.O. Tam, et al., Multicolored silver nanoparticles for multiplexed disease diagnostics: distinguishing dengue, yellow fever, and Ebola viruses, *Lab Chip* 15 (2015) 1638–1641.
- [20] P.J. Lamas-Ardisana, G. Martínez-Paredes, L. Añorga, et al., Glucose biosensor based on disposable electrochemical paper-based transducers fully fabricated by screen-printing, *Biosens. Bioelectron.* 109 (2018) 8–12.
- [21] E.L. Rossini, M.I. Milani, E. Carrilho, et al., Simultaneous determination of renal function biomarkers in urine using a validated paper-based microfluidic analytical device, *Anal. Chim. Acta* 997 (2018) 16–23.
- [22] X. Weng, S.R. Ahmed, S. Neethirajan, A nanocomposite-based biosensor for bovine haptoglobin on a 3D paper-based analytical device, *Sensor. Actuator. B Chem.* 265 (2018) 242–248.
- [23] R.W. Peeling, K.K. Holmes, D. Mabey, et al., Rapid tests for sexually transmitted infections (STIs): the way forward, *Sex. Transm. Infect.* 82 (2006) v1–v6.
- [24] A.W. Martinez, S.T. Phillips, G.M. Whitesides, et al., Diagnostics for the developing world: microfluidic paper-based analytical devices, *Anal. Chem.* 82 (2010) 3–10.
- [25] E. Sharpe, R. Bradley, T. Frasco, et al., Metal oxide based multisensor array and portable database for field analysis of antioxidants, *Sensor. Actuator. B Chem.* 193 (2014) 552–562.
- [26] N. Nuchtavorn, M. Macka, A novel highly flexible, simple, rapid and low-cost fabrication tool for paper-based microfluidic devices (μ PADs) using technical drawing pens and in-house formulated aqueous inks, *Anal. Chim. Acta* 919 (2016) 70–77.
- [27] S.X. Guo, J.Y. Shao, Y. Wang, et al., Detection of antioxidant activity of Danhong injection and its intermediate with a paper-based analytical device, *China J. Chin. Mater. Med.* 43 (2018) 1851–1856.
- [28] S.X. Guo, J.Y. Shao, X.C. Gong, Paper-based analytical devices prepared with polycaprolactone printing and their application in the activity determination of mulberry extracts, *J. Pharmaceut. Biomed. Anal.* 161 (2018) 28–34.
- [29] P. Rchette, T. Bardin, Gout, *Lancet* 375 (2009) 318–328.
- [30] W.J. Chen, Y. Wu, X. Zhao, et al., Screening the anti-gout traditional herbs from TCM using an in vitro method, *Chin. Chem. Lett.* 27 (2016) 1701–1707.
- [31] L. Guan, R. Cao, J. Tian, et al., A preliminary study on the stabilization of blood typing antibodies sorbed into paper, *Cellulose* 21 (2014) 717–727.
- [32] S. Ramachandran, E. Fu, B. Lutz, et al., Long-term dry storage of an enzyme-based reagent system for ELISA in point-of-care devices, *Analyst* 139 (2014) 1456–1462.
- [33] T. Niu, B. Xu, H. Chen, et al., Determination of monosaccharide and disaccharide in tanshinon extract by HPLC-ELSD, *Chin. J. Mod. Appl. Pharm.* 30 (2013) 183–186.
- [34] X.Y. Liu, R.H. Chen, Y.J. Shang, et al., Superoxide radicals scavenging and xanthine oxidase inhibitory activity of magnesium lithospermate B from *Salvia miltiorrhiza*, *J. Enzym. Inhib. Med. Chem.* 24 (2009) 663–668.